

Ptychographic imaging and micromagnetic modeling of thermal melting of nanoscale magnetic domains in antidot lattices F

Cite as: AIP Advances **10**, 125122 (2020); <https://doi.org/10.1063/5.0025784>

Submitted: 18 August 2020 • Accepted: 11 November 2020 • Published Online: 17 December 2020

 Joachim Gräfe, Maxim Skripnik, Georg Dieterle, et al.

COLLECTIONS

F This paper was selected as Featured



View Online



Export Citation



CrossMark

ARTICLES YOU MAY BE INTERESTED IN

[Soft x-ray ptychography studies of nanoscale magnetic and structural correlations in thin SmCo₅ films](#)

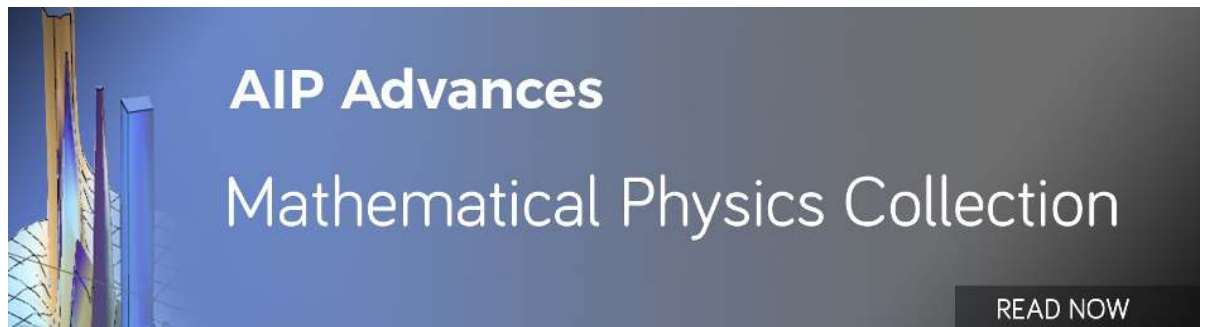
Applied Physics Letters **108**, 094103 (2016); <https://doi.org/10.1063/1.4942776>

[X-ray ptychography on low-dimensional hard-condensed matter materials](#)

Applied Physics Reviews **6**, 011306 (2019); <https://doi.org/10.1063/1.5045131>

[The design and verification of MuMax3](#)

AIP Advances **4**, 107133 (2014); <https://doi.org/10.1063/1.4899186>

















Ptychographic imaging and micromagnetic modeling of thermal melting of nanoscale magnetic domains in antidot lattices

Cite as: AIP Advances 10, 125122 (2020); doi: 10.1063/5.0025784

Submitted: 18 August 2020 • Accepted: 11 November 2020 •

Published Online: 17 December 2020



Joachim Gräfe,^{1,a)}  Maxim Skripnik,^{2,3}  Georg Dieterle,¹  Felix Haering,⁴  Markus Weigand,¹  Iuliia Bykova,¹  Nick Träger,¹  Hermann Stoll,^{1,5}  Tolek Tylliszczak,⁶  David Vine,⁶  Paul Ziemann,⁴  Ulf Wiedwald,⁷  David Shapiro,⁶  Ulrich Nowak,²  Gisela Schütz,¹ and Eberhard J. Goering¹

AFFILIATIONS

¹Max Planck Institute for Intelligent Systems, 70569 Stuttgart, Germany

²Department of Physics, Universität Konstanz, 78464 Konstanz, Germany

³Okinawa Institute of Science Technology Graduate University, 904-0495 Okinawa, Japan

⁴Institute of Solid State Physics, Ulm University, 89081 Ulm, Germany

⁵Institute of Physics, Johannes Gutenberg University, 55122 Mainz, Germany

⁶Lawrence Berkeley National Laboratory, Berkeley, California 94720, USA

⁷Faculty of Physics and Center for Nanointegration (CENIDE), University of Duisburg-Essen, 47057 Duisburg, Germany

^{a)} Author to whom correspondence should be addressed: graefe@is.mpg.de

ABSTRACT

Antidot lattices are potential candidates to act as bit patterned media for data storage as they are able to trap nanoscale magnetic domains between two adjacent holes. Here, we demonstrate the combination of micromagnetic modeling and x-ray microscopy. Detailed simulation of these systems can only be achieved by micromagnetic modeling that takes thermal effects into account. For this purpose, a Landau–Lifshitz–Bloch approach is used here. The calculated melting of magnetic domains within the antidot lattice is reproduced experimentally by x-ray microscopy. Furthermore, we compare conventional scanning transmission x-ray microscopy with resolution enhanced ptychography. Hence, we achieve a resolution of 13 nm. The results demonstrate that ptychographic imaging can also recover magnetic contrast in the presence of a strong topological variation and is generally applicable toward magnetic samples requiring ultimate resolution.

© 2020 Author(s). All article content, except where otherwise noted, is licensed under a Creative Commons Attribution (CC BY) license (<http://creativecommons.org/licenses/by/4.0/>). <https://doi.org/10.1063/5.0025784>

I. INTRODUCTION

With the miniaturization of magnetic systems for device applications, the need for nanoscale modeling and imaging increases. In technologically relevant structures, proper modeling of thermal effects is of great importance to predict performance parameters. A suitable approach for micromagnetic modeling is the so called Landau–Lifshitz–Bloch (LLB) equation that was derived from the Fokker–Planck equation by Garanin in 1997.¹ This extension of the common Landau–Lifshitz–Gilbert equation allows for a variation in the macrospin magnitude and temperature dependent damping.²

In turn, these micromagnetic descriptions can be verified by microscopic techniques, whereas the resolution of x-ray microscopy makes this technique especially suitable for experimental investigations.^{3–5} However, the resolution of scanning transmission x-ray microscopy (STXM) is not wavelength limited, but it is limited by the performance of x-ray optics.⁶ The introduction of ptychography for x-ray imaging overcame this limitation and resolutions below 10 nm have been achieved for chemical contrast.^{3,6–8} While STXM acquires an integrated transmitted intensity per illumination spot [illustrated in Fig. 1(a)], ptychography is a coherent diffractive imaging technique that makes use of the diffraction pattern generated by the sample.^{8,9} Therefore, a full diffraction pattern is acquired for

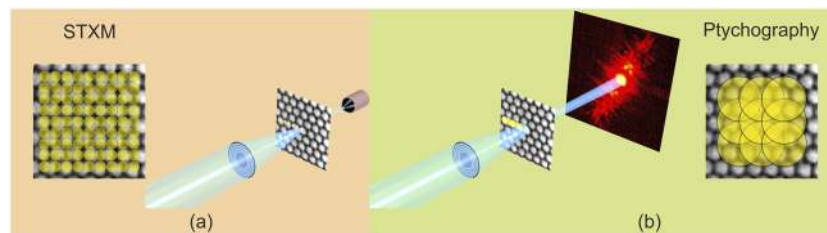


FIG. 1. Soft x-ray schemes for magnetic imaging: (a) scanning transmission x-ray imaging illuminates a fine grid of pixels and acquires the integrated transmitted intensity, and its resolution relies on the smallest focal size achieved by the x-ray optics and (b) ptychography has a larger illumination spot and probes overlapping areas while acquiring a full diffraction pattern for each spot; its resolution relies on the largest detected diffraction angle.

each illumination spot [illustrated in Fig. 1(b)]. When these illumination spots overlap sufficiently, the amplitude and phase information of the sample's transmission and the illumination probe function can be calculated using an iterative algorithm.^{7–12} While this works exceptionally well for chemically resonant charge contrast, the resolution enhancement for magnetic samples is limited.^{13,14} This can also be attributed to the fact that the magnetic scattering contrast is two orders of magnitude smaller than the magnetic absorption contrast.⁷ Hence, so far, ptychography has only been rarely used for imaging magnetic samples.^{8,13–19} However, the reconstruction of the illumination probe function and the phase information still results in increased microcontrast and resolution when pushing the limits of x-ray microscopy.^{3,13,14}

One example of an application of nanoscale magnetic structures is data storage. The areal density of magnetic storage media has continuously been increased since the introduction of magnetic hard disk drives in 1956.^{20,21} However, in recent years, the annual improvement has slowed down,²¹ mainly limited by thermal effects or superparamagnetism, which leads to information loss.^{20,22–25} In conventional recording media, a sufficient number of grains per bit is needed to achieve a sufficient signal to noise ratio (SNR). However, thermally activated switching leads to information loss if these grains get too small and if $K_u \cdot V/k_B \cdot T$ drops below 60, where K_u is the anisotropy, V is the magnetic switching volume, k_B is the Boltzmann constant, and T is the temperature.^{20,23,26} To circumvent the need for multiple grains per bit to improve the SNR, the so called bit patterned media (BPM) were used, where a bit is constituted by a lithographically defined and uniformly magnetized volume.²⁰ However, BPM consisting of magnetic islands as individual bits suffer from broadening of their switching field distribution (SFD) due to dipolar coupling between neighbors.^{21,27,28} This could possibly be circumvented by exchange coupled composites²¹ which has the additional advantage of avoiding the superparamagnetic limit for individual islands.^{29,30} Systems that could potentially fulfill these requirements are the so called antidot lattices (ADLs), i.e., a periodic arrangement of holes in a magnetic thin film that can be easily produced by colloidal lithography.^{31,32} This method has first been proposed by Sun *et al.*,³³ and recording densities in the Tb/in² range can be reached.³⁴

Here, we study an ADL to demonstrate the interplay between LLB simulations and x-ray microscopy. To this end, we investigate the melting of the smallest magnetic domains in an ADL by micromagnetic modeling including thermal effects and verify these

with x-ray microscopy and x-ray ptychography to demonstrate LLB modeling and the power of magnetic soft x-ray ptychography.

II. METHODS

The antidot lattices were produced by nanosphere lithography using commercial polystyrene (PS) nanospheres.^{31,35} Closely packed monolayers of these PS spheres are deposited on Si₃N₄ (500 nm, membranes)/Si(100) substrates by dip coating. Details of this preparation procedure can be found elsewhere.^{36,37} The deposited PS spheres were etched by an oxygen plasma to reduce their diameter. The nominal center to center distance of the PS spheres was set to 200 nm, and their diameter was set to 160 nm. On top of these templates, GdFe [0.36/0.36 nm] multilayer films were deposited with a 2 nm Al capping layer under UHV conditions by ion beam sputtering.³⁸ The total film thickness was set to 45 nm (60× GdFe).^{4,5,39} Finally, the PS spheres were removed by chemo-mechanical polishing to reveal the ADL. Fe and Gd are generally subjected to oxidation. Although the initial oxidation rate of pure Fe is very high, oxide formation quickly saturates, forming a passivated surface.⁴⁰ Degradation of the GdFe multilayer system would lead to a loss of perpendicular magnetic anisotropy, which was not observed during patterning or storage. As the perpendicular anisotropy of the antidot lattice samples was unaffected over the course of several weeks, we suppose that a very thin oxide layer formed on the hole rims and prevented further oxidation.⁵

SXM measurements were conducted at the MAXYMUS end station at the UE46-PGM2 beam line at the BESSY II synchrotron radiation facility. The samples were illuminated under normal incidence by circularly polarized light in an applied out-of-plane field of up to 240 mT that was generated by a set of four rotatable permanent magnets.⁴¹ The photon energy was set to the absorption maximum of the Fe *L*₃ edge to get optimal X-ray Magnetic Circular Dichroism (XMCD) contrast for imaging.^{4,5,39}

Ptychography measurements were conducted at beamline 11.0.2. of the Advanced Light Source. The samples were illuminated under normal incidence by circularly polarized light in a remanent magnetization state and zero applied field. The photon energy was set to the absorption maximum of the Fe *L*₃ edge to get maximum XMCD contrast in absorption. A detailed description of the diffraction acquisition setup and the SHARP software, a graphics processing unit (GPU) accelerated ptychographic reconstruction algorithm, can be found elsewhere.^{6,12} For calculation of the XMCD images,

the absorption contrast of the ptychographic reconstruction was used.

The transmission through the holes with no x-ray absorption other than from the Si_3N_4 membrane served as an internal I_0 intensity reference to normalize the measured intensities to the incident beam intensity. Intensities were locally averaged using a Gaussian filter in ImageJ.⁴² Images taken at different photon helicities were registered using ImageJ with TurboReg⁴³ to align the individual images.^{4,5,39}

Micromagnetic simulations were conducted using a custom implementation of the Landau–Lifshitz–Bloch equation based on the OpenCL framework using GPUs to solve the equation of motion.⁴⁴ Finite temperatures were implemented as normally distributed random thermal noise.²⁵ The custom code was verified against μMAG standard problems 3 and 4.⁴⁵ The antidot lattice was discretized into $14 \times 14 \times 14 \text{ nm}^3$ cells, and as material parameters, the saturation magnetization at zero temperature $M_0 = 3.72 \times 10^5 \text{ A m}^{-1}$, the uniaxial anisotropy constant $K_u = 1.2 \times 10^5 \text{ J m}^{-3}$, and the exchange stiffness at 300 K $A(300 \text{ K}) = 7.78 \times 10^{-11} \text{ J m}^{-1}$ were assumed.⁴⁵ In addition, 5% of the macrospins were given an arbitrary magnetization and orientation to include some irregularity of the real samples into the simulations.

III. RESULTS

The general structure of the thin GdFe film hosting an ADL that was used as the model system here is shown in Fig. 2(a). Furthermore, Fig. 2(b) shows micromagnetic simulations for this structure at temperatures of 50 K, 300 K, 400 K, and 450 K. In the ADL, the domain walls tend to be located at the shortest distance between two adjacent holes to minimize the exchange energy associated with the domain wall.^{4,5,30} This is also observed in simulations, especially at low temperatures (50 K). As shown in Fig. 2(c), such a trapped domain between two holes is shown in more detail. In a BPM application, these domains would act as individual bits of

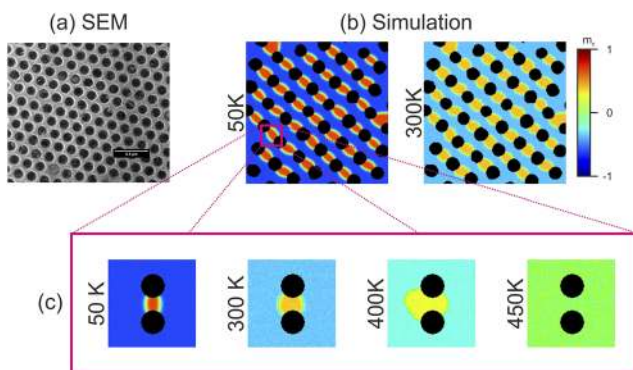


FIG. 2. (a) SEM image of the sample structure and the result of the (b) micromagnetic simulation of a GdFe thin film with an antidot lattice. The domain walls tend to span the shortest distance between two adjacent holes, i.e., trapping domains between two holes. The expansion (c) shows the temperature dependence of the structure of a trapped domain. With increasing thermal activation, the domain walls smear out and move away from the holes, resembling a melting process, until the Curie temperature is reached and all magnetic structures vanish.

the storage medium. Upon increasing the temperature (300 K and 400 K), thermal activation leads to an elongation of the domain walls, and the domains start to smear out, resembling melting of the ordered domains.⁴⁶ While exact estimation of the temperature dependent material parameters is still challenging, a strong influence of the temperature can be seen qualitatively. It is evident that the domain shape becomes more irregular with the increase in temperature. At elevated temperatures, the domains extend beyond the constriction between two holes and deforms.

Figure 3(a) shows STXM measurements that were carried out to reproduce these results.⁵ Unfortunately, the resolution and micro-contrast of zone plate limited x-ray microscopy do not allow evaluation of the domain shape, and only the existence of a domain trapped between two adjacent holes can be confirmed, as illustrated below the micrograph in Fig. 3(a).

Thus, additional ptychography measurements were carried out on the same samples, and the absorption contrast is shown in Fig. 3(b). With enhanced resolution and contrast of ptychography, the fine structure of the trapped domain could be elaborated, which is sketched in Fig. 3(b). A clear melting of the domain can be observed, with domain walls deviating from the shortest distance between the two holes. Furthermore, there is a strong resemblance to the micromagnetic simulation [cf. Figure 2(c)] at elevated temperatures that shows the same behavior of the magnetic structure. This strongly indicates that thermal effects cannot be neglected for proper modeling of room temperature magnetization landscapes on the nanoscale. However, this could only be experimentally resolved by ptychographic resolution enhancement. While STXM only allows detection of a magnetic domain in general, the increased resolution achieved by ptychography yields insights into the exact shape of the domain.

Beyond the qualitative discussion, we quantify the resolution enhancement achieved in ptychography compared to STXM.

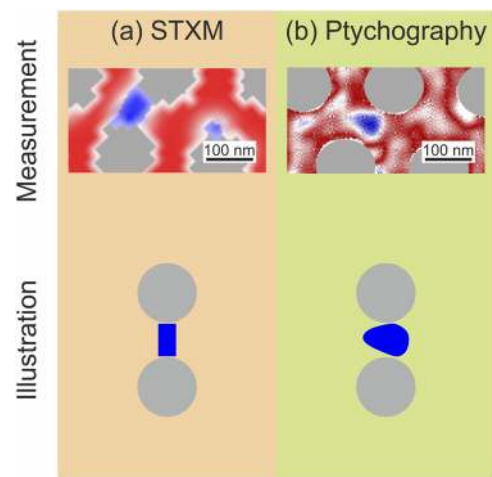


FIG. 3. Comparison of the magnetic contrast of a thin GdFe film hosting an ADL seen by (a) STXM and (b) ptychography (absorption contrast) at room temperature. In the coarser STXM image, no fine contrast is visible, while the ptychography image shows smearing out of the domain that is trapped between two holes, resembling the micromagnetic simulation at non-zero temperature.

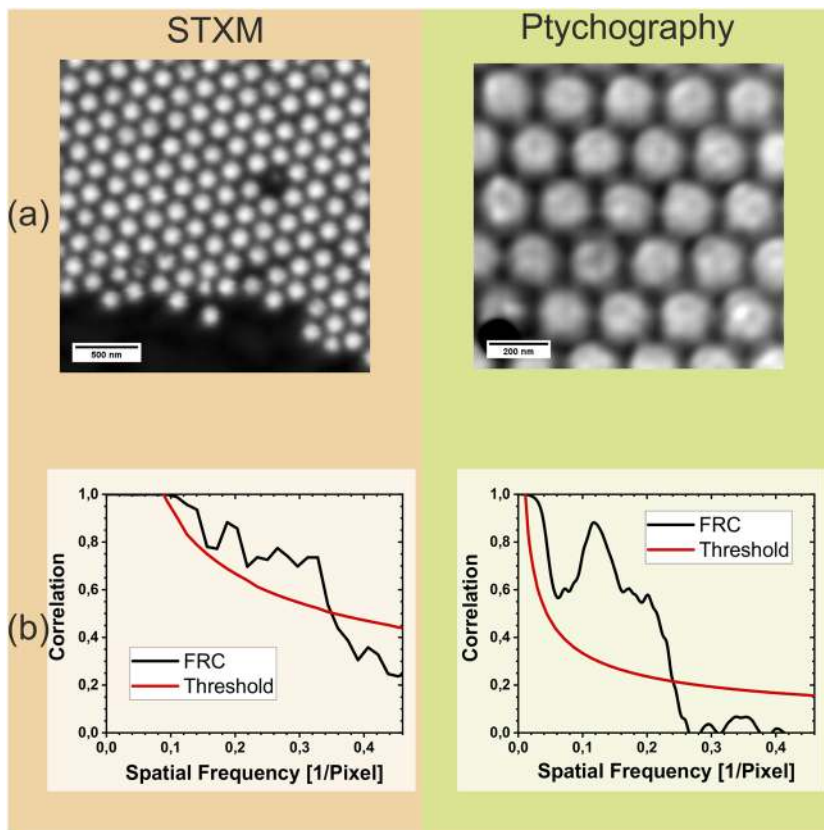


FIG. 4. (a) X-ray micrographs of a thin GdFe film hosting an ADL acquired by STXM and ptychography (absorption contrast). Furthermore, (b) the Fourier ring correlations and 3σ threshold are shown, indicating a resolution of 57 nm for STXM and 13 nm for ptychography.

Figure 4(a) shows the STXM and ptychography images that were used to calculate the magnetic contrast. For these, the Fourier ring correlation (FRC) was calculated and is shown with the 3σ threshold in Fig. 4(b).^{47,48} The calculated resolutions were 57 nm for STXM and 13 nm for ptychography, further justifying the enhanced microcontrast observed for the latter. Both values are plausible, considering the respective scan parameters and the typical resolutions achieved for similar materials.^{3,5,13,14,19} It is noteworthy that FRC is a resolution criterion based on the final image, i.e., it depends on the optical resolution, measurement settings, and signal to noise ratio and the structural features of the sample. Furthermore, the Fourier analysis depends on the chosen pixel size that favors oversampled images. Thus, the resolutions achieved here may not be the ultimate resolution achievable with the respective methods, but it is a good indication for routinely achievable values. In addition, one has to consider the illumination time per sample area that was $50 \mu\text{s nm}^{-2}$ for STXM and $250 \mu\text{s nm}^{-2}$ for ptychography. Thus, an approximate factor of five in resolution enhancement comes at the cost of a factor of five in measurement time.

While ptychography can achieve single nanometer resolution for chemical contrast, XMCD contrast typically yields a lower resolution and is hence less used in magnetic imaging.^{3,13,19} This is due to the reduced scattering power of magnetic contrast in comparison to charge contrast.^{49,50} Another challenge for ptychography is competing scattering contrasts, e.g., topological vs magnetic contrast

that may prevent proper reconstruction. Hence, previous investigations by others focused on uniform thin films when imaging magnetic domains.^{13,19} However, we show here that recovery of magnetic information is possible without resolution penalties despite the presence of a strong topological contrast, i.e., ptychography can be used for magnetic imaging without limitations.

IV. SUMMARY

We have investigated nanoscale magnetic ADLs that could potentially be applied as BPM for high area density storage media, where we focused on detailed modeling and imaging of a single bit. It was shown that inclusion of thermal effects, using an LLB approach, is important for capturing the actual structure of the magnetic domains, e.g., the storage bits. Thermal melting, i.e., smearing out, of magnetic domains trapped between two holes was observed. Furthermore, we have confirmed the micromagnetic modeling with nanoscopic imaging. While the structure was beyond the resolution limit of conventional STXM, ptychographic imaging could provide sufficient resolution and microcontrast to yield a sharp image of the magnetic domains. Thus, overcoming the limitations of x-ray imaging by ptychographic approaches is also possible for magnetic samples. At the same time, we showed that ptychographic reconstruction of magnetic contrast is also possible in the presence of strong topological contrast, i.e., a secondary scattering contrast can

also be recovered in the presence of a stronger scattering effect. This opens up this x-ray microscopy enhancement to more complex sample systems.

ACKNOWLEDGMENTS

The authors would like to thank Michael Bechtel for support during beam times and Bernd Ludescher for thin film deposition. Furthermore, we are grateful to Ulrike Eigenthaler for performing SEM measurements. Helmholtz Zentrum Berlin is acknowledged for allocating beam time at the BESSY II synchrotron radiation facility. Financial support by the Baden-Württemberg Stiftung in the framework of the Kompetenznetz Funktionelle Nanostrukturen is gratefully acknowledged. The data that support the findings of this study are available from the corresponding author upon reasonable request.

REFERENCES

- D. A. Garanin, *Phys. Rev. B* **55**, 3050 (1997).
- U. Atxitia, D. Hinzke, and U. Nowak, *J. Phys. D: Appl. Phys.* **50**, 033003 (2016).
- A. P. Hitchcock, *J. Electron Spectrosc. Relat. Phenom.* **200**, 49 (2015).
- J. Gräfe, M. Weigand, C. Stahl, N. Träger, M. Kopp, G. Schütz, E. J. Goering, F. Haering, P. Ziemann, and U. Wiedwald, *Phys. Rev. B* **93**, 014406 (2016).
- J. Gräfe, M. Weigand, N. Träger, G. Schütz, E. J. Goering, M. Skripnik, U. Nowak, F. Haering, P. Ziemann, and U. Wiedwald, *Phys. Rev. B* **93**, 104421 (2016).
- D. A. Shapiro, Y.-S. Yu, T. Tyliczszak, J. Cabana, R. Celestre, W. Chao, K. Kaznatcheev, A. L. D. Kilcoyne, F. Maia, S. Marchesini, Y. S. Meng, T. Warwick, L. L. Yang, and H. A. Padmore, *Nat. Photonics* **8**, 765 (2014).
- P. Thibault, M. Dierolf, A. Menzel, O. Bunk, C. David, and F. Pfeiffer, *Science* **321**, 379 (2008).
- X. Zhu, A. P. Hitchcock, D. A. Bazylinski, P. Denes, J. Joseph, U. Lins, S. Marchesini, H.-W. Shiu, T. Tyliczszak, and D. A. Shapiro, *Proc. Natl. Acad. Sci. U. S. A.* **113**, E8219 (2016).
- P. Thibault, M. Guizar-Sicairos, and A. Menzel, *J. Synchrotron Radiat.* **21**, 1011 (2014).
- P. Thibault, M. Dierolf, O. Bunk, A. Menzel, and F. Pfeiffer, *Ultramicroscopy* **109**, 338 (2009).
- J. Donatelli, M. Haranczyk, A. Hexemer, H. Krishnan, X. Li, L. Lin, F. Maia, S. Marchesini, D. Parkinson, T. Perciano, D. Shapiro, D. Ushizima, C. Yang, and J. A. Sethian, *Synchrotron Radiat. News* **28**, 4 (2015).
- S. Marchesini, H. Krishnan, B. J. Daurer, D. A. Shapiro, T. Perciano, J. A. Sethian, and F. R. N. C. Maia, *J. Appl. Crystallogr.* **49**, 1245 (2016).
- X. Shi, P. Fischer, V. Neu, D. Elefant, J. C. T. Lee, D. A. Shapiro, M. Farmand, T. Tyliczszak, H.-W. Shiu, S. Marchesini, S. Roy, and S. D. Kevan, *Appl. Phys. Lett.* **108**, 094103 (2016).
- C. Donnelly, V. Scagnoli, M. Guizar-Sicairos, M. Holler, F. Wilhelm, F. Guillou, A. Rogalev, C. Detlefs, A. Menzel, J. Raabe, and L. J. Heyderman, *Phys. Rev. B* **94**, 064421 (2016).
- D. Tripathy and A. O. Adeyeye, *New J. Phys.* **13**, 023035 (2011).
- P. Fischer, *Nature* **547**, 290 (2017).
- C. Donnelly, M. Guizar-Sicairos, V. Scagnoli, S. Gliga, M. Holler, J. Raabe, and L. J. Heyderman, *Nature* **547**, 328 (2017).
- Y.-S. Yu, R. Celestre, B. Enders, K. Nowrouzi, H. Padmore, T. Warwick, J.-R. Jeong, and D. A. Shapiro, *Microsc. Microanal.* **24**, 530 (2018).
- W. Li, I. Bykova, S. Zhang, G. Yu, R. Tomasello, M. Carpentieri, Y. Liu, Y. Guang, J. Gräfe, M. Weigand, D. M. Burn, G. van der Laan, T. Hesjedal, Z. Yan, J. Feng, C. Wan, J. Wei, X. Wang, X. Zhang, H. Xu, C. Guo, H. Wei, G. Finocchio, X. Han, and G. Schütz, *Adv. Mater.* **31**, 1807683 (2019).
- B. D. Terris and T. Thomson, *J. Phys. D: Appl. Phys.* **38**, R199 (2005).
- T. R. Albrecht, H. Arora, V. Ayanoor-Vitikatte, J. Beaujour, D. Bedau, D. Berman, A. L. Bogdanov, Y.-A. Chapuis, J. Cushen, E. E. Dobisz, G. Doerk, H. Gao, M. Grobis, B. Gurney, W. Hanson, O. Hellwig, T. Hirano, P. Jubert, D. Kercher, J. Lille, Z. Liu, C. M. Mate, Y. Obukhov, K. C. Patel, K. Rubin, R. Ruiz, M. Schabes, L. Wan, D. Weller, T. Wu, and E. Yang, *IEEE Trans. Magn.* **51**, 0800342 (2015).
- S. H. Charap, L. Pu-Ling, and H. Yanjun, *IEEE Trans. Magn.* **33**, 978 (1997).
- D. Weller and A. Moser, *IEEE Trans. Magn.* **35**, 4423 (1999).
- A. Moser, K. Takano, D. T. Margulies, M. Albrecht, Y. Sonobe, Y. Ikeda, S. Sun, and E. E. Fullerton, *J. Phys. D: Appl. Phys.* **35**, R157 (2002).
- R. F. L. Evans, D. Hinzke, U. Atxitia, U. Nowak, R. W. Chantrell, and O. Chubykalo-Fesenko, *Phys. Rev. B* **85**, 014433 (2012).
- R. F. L. Evans, R. W. Chantrell, U. Nowak, A. Lyberatos, and H.-J. Richter, *Appl. Phys. Lett.* **100**, 102402 (2012).
- B. Pfau, C. M. Günther, E. Guehrs, T. Hauet, H. Yang, L. Vinh, X. Xu, D. Yaney, R. Rick, S. Eisebitt, and O. Hellwig, *Appl. Phys. Lett.* **99**, 062502 (2011).
- B. Pfau, C. M. Günther, E. Guehrs, T. Hauet, T. Hennen, S. Eisebitt, and O. Hellwig, *Appl. Phys. Lett.* **105**, 132407 (2014).
- R. P. Cowburn, A. O. Adeyeye, and J. A. C. Bland, *Appl. Phys. Lett.* **70**, 2309 (1997).
- J. Gräfe, G. Schütz, and E. J. Goering, *J. Magn. Magn. Mater.* **419**, 517 (2016).
- U. Wiedwald, F. Haering, S. Nau, C. Schulze, H. Schletter, D. Makarov, A. Plettl, K. Kuepper, M. Albrecht, J. Boneberg, and P. Ziemann, *Beilstein J. Nanotechnol.* **3**, 831 (2012).
- U. Wiedwald, J. Gräfe, K. M. Lebecki, M. Skripnik, F. Haering, G. Schütz, P. Ziemann, E. Goering, and U. Nowak, *Beilstein J. Nanotechnol.* **7**, 733 (2016).
- S. Sun, C. B. Murray, D. Weller, L. Folks, and A. Moser, *Science* **287**, 1989 (2000).
- D. V. Talapin, J.-S. Lee, M. V. Kovalenko, and E. V. Shevchenko, *Chem. Rev.* **110**, 389 (2010).
- A. Plettl, F. Enderle, M. Saitner, A. Manzke, C. Pfahler, S. Wiedemann, and P. Ziemann, *Adv. Funct. Mater.* **19**, 3279 (2009).
- F. Haering, U. Wiedwald, T. Häberle, L. Han, A. Plettl, B. Koslowski, and P. Ziemann, *Nanotechnology* **24**, 055305 (2013).
- F. Haering, U. Wiedwald, S. Nothelfer, B. Koslowski, P. Ziemann, L. Lechner, A. Wallucks, K. Lebecki, U. Nowak, J. Gräfe, E. Goering, and G. Schütz, *Nanotechnology* **24**, 465709 (2013).
- E. Amaladass, B. Ludescher, G. Schütz, T. Tyliczszak, and T. Eimüller, *Appl. Phys. Lett.* **91**, 172514 (2007).
- J. Gräfe, F. Haering, T. Tietze, P. Audehm, M. Weigand, U. Wiedwald, P. Ziemann, P. Gawronski, G. Schütz, and E. J. Goering, *Nanotechnology* **26**, 225203 (2015).
- R. Davies, D. Edwards, J. Gräfe, L. Gilbert, P. Davies, G. Hutchings, and M. Bowker, *Surf. Sci.* **605**, 1754 (2011).
- D. Nolle, M. Weigand, P. Audehm, E. Goering, U. Wiesemann, C. Wolter, E. Nolle, and G. Schütz, *Rev. Sci. Instrum.* **83**, 046112 (2012).
- W. Rasband, ImageJ, 1997–2015.
- P. Thevenaz, U. E. Ruttimann, and M. Unser, *IEEE Trans. Image Process.* **7**, 27 (1998).
- N. Kazantseva, D. Hinzke, U. Nowak, R. W. Chantrell, U. Atxitia, and O. Chubykalo-Fesenko, *Phys. Rev. B* **77**, 184428 (2008).
- M. Skripnik, “Controlling the magnetic structure in antidot arrays: A numerical study,” M. Sc. thesis, University of Konstanz, 2014.
- V. A. Zablotskii and Y. A. Mamalui, *J. Phys.: Condens. Matter* **7**, 5271 (1995).
- R. P. J. Nieuwenhuizen, K. A. Lidke, M. Bates, D. L. Puig, D. Grünwald, S. Stallinga, and B. Rieger, *Nat. Methods* **10**, 557 (2013).
- N. Banterle, K. H. Bui, E. A. Lemke, and M. Beck, *J. Struct. Biol.* **183**, 363 (2013).
- M. Blume, *J. Appl. Phys.* **57**, 3615 (1985).
- I. Bykova, “High-resolution X-ray ptychography for magnetic imaging,” Ph.D. thesis, Universität Stuttgart, 2018.